REFERENCES AND NOTES

1. R. Schleif, in Escherchia coli *and* Salmonella Typhimurium, F. Neidhardt *et al*., Eds. (American Society for Microbiology, Washington, DC, 1996), pp. 1300–1309.
2. T. Dunn, S. Hahn, S. Ogden , R. Schleif, *Proc. Natl. Acad. Sci. U.S.A.* **81**, 5017 (1984).
3. K. Martin, L. Huo, R. Schleif, *ibid.* **83**, 3654 (1986).
4. R. Lobell and R. Schleif, *Science* **250**, 528 (1990).
5. W. Hendrickson and R. Schleif, *Proc. Natl. Acad. Sci. U.S.A.* **82**, 3129 (1985).
6. _____, *J. Mol. Biol.* **178**, 611 (1984).
7. X. Zhang, T. Reeder, R. Schleif, *ibid.* **258**, 14 (1996).
8. R. Schleif, *Annu. Rev. Biochem.* **61**, 199 (1992).
9. S. Bustos and R. Schleif, *Proc. Natl. Acad. Sci. U.S.A.* **90**, 5638 (1993).
10. R. Eustance, S. Bustos, R. Schleif, *J. Mol. Biol.* **242**, 330 (1994).
11. H. Lauble, Y. Georgalis, U. Heinemann, *Eur. J. Biochem.* **185**, 319 (1989).
12. R. Eustance and R. Schleif, *J. Bacteriol.* **178**, 7025 (1996).
13. G. Wilcox and P. Meuris, *Mol. Gen. Genet.* **145**, 97 (1976).
14. J. Carra and R. Schleif, *EMBO J*. **12**, 35 (1993).
15. Intact AraC was expressed in *E. coli* and purified [R. Schleif and A. Favreau, *Biochemistry* **21**, 778 (1982)]. After dialyzing purified protein into buffer A [15 mM tris-HCl (pH 8.0), 75 mM KCl, 0.2% (w/v) L-arabinose], we prepared a tryptic fragment comprising the NH_2-terminal two-thirds of the protein by digesting intact AraC overnight with 0.1% trypsin by mass. The cleavage mixture was concentrated by ultrafiltration, and the NH_2-terminal domain was purified by anion-exchange chromatography on a Mono-Q column (Pharmacia, Uppsala, Sweden) developed with a gradient of buffer A + 1 M KCl. Peak fractions were dialyzed into buffer A + 2 mM sodium azide, concentrated by ultrafiltration to 8 to 12 mg/ml, and stored at 4°C. Arabinose was added to a final concentration of 0.2% (w/v) immediately before cocrystallization by hanging-drop vapor diffusion. Amino-terminal sequencing and matrix-assisted laser desorption/ionization time-of-flight mass spectrometry indicated that the tryptic fragment was >99% pure and contained residues 2 to 178 of AraC (S. Soisson, unpublished data). Small, blocky crystals appear infrequently with a reservoir solution of 30% (w/v) polyethylene glycol (PEG) 8000, 100 mM tris-HCl (pH 7.0), and 40 mM $MgCl_2$. Optimal results were obtained when crystals were grown by microseeding, with a reservoir solution containing 18% PEG 8000, 100 mM tris-HCl (pH 7.25), and 40 mM magnesium acetate. All cocrystals of AraC and arabinose were initially stabilized in a solution of 24% PEG 8000, 100 mM tris-HCl (pH 7.5), 40 mM magnesium acetate, and 0.2% (w/v) L-arabinose. For data collection, crystals were transferred to the above stabilizing solution plus 10% PEG 400 for 5 to 10 min and then flash-frozen in a small monofilament nylon loop placed in a cold nitrogen stream maintained at 100 K.
16. Crystals of the sugar-binding and dimerization domain of AraC in the absence of arabinose were grown by hanging-drop vapor diffusion with a reservoir solution of 20% PEG 4000, 0.1 M tris-HCl (pH 9.0), 5 mM KCl, and 0.2 M sodium acetate. Crystals were stabilized by sequential transfer into reservoir solutions containing increasing amounts of PEG 4000 in 4% increments (10 min in each step) until a concentration of 40% PEG 4000 was reached. Crystals were then directly flash-frozen in a 100 K nitrogen stream for data collection.
17. Simulated-annealing omit maps calculated with X-PLOR consistently showed the presence of only the α-anomer of L-arabinose in the AraC binding site. The equilibrium dissociation constant of *E. coli* AraC and arabinose is $\sim 10^{-3}$ M [G. Wilcox, *J. Biol. Chem.* **249**, 6892 (1974)].
18. Accessible surface area calculations were performed with X-PLOR, and probe sizes of 1.4, 1.5, and 1.6 Å gave similar results.
19. F. H. C. Crick, *Acta Crystallogr.* **6**, 689 (1953).
20. Modeled as a water, the molecule has a refined thermal B factor of 14.4 $Å^2$ and an occupancy of 1.0, as compared with an average B factor of 26.6 $Å^2$ for all water molecules. This does not exclude the possibility that the "water" is a sodium or potassium ion.
21. W. S. Somers and S. E. V. Phillips, *Nature* **359**, 387 (1992).
22. J. Janin and F. Rodier, *Proteins* **23**, 580 (1995).
23. S. M. Soisson, B. MacDougall-Shackleton, R. Schleif, C. Wolberger, data not shown.
24. G. D. V. Duyne, G. Ghosh, W. K. Maas, P. B. Sigler, *J. Mol. Biol.* **256**, 377 (1996).
25. N. Lee, C. Francklyn, E. Hamilton, *Proc. Natl. Acad. Sci. U.S.A.* **84**, 8814 (1987).
26. Z. Otwinowski, Oscillation Data Reduction Program, L. Sawyer, N. Isaacs, S. Bailey, Eds., *Proceedings of the CCP4 Study Weekend: Data Collection and Processing* (SERC Daresbury Laboratory, 1993).
27. Collaborative Computational Project Number 4, *Acta Crystallogr.* **D50**, 760 (1994).
28. T. A. Jones, J. Y. Zou, S. W. Cowan, M. Kjeldgaard, *ibid.* **A47**, 110 (1991).
29. A. T. Brünger, *X-PLOR v3.1, A System for X-Ray Crystallography and NMR*, *Manual* (Yale Univ. Press, New Haven, CT, 1992).
30. After two rounds of simulated annealing and positional refinement in X-PLOR, one molecule of α-L-arabinose per monomer was added. The model was completed by alternating rounds of Powell positional refinement in X-PLOR followed by manual adjustments. The rmsd for superimposed monomers (A and B) of AraC in the asymmetric unit is 0.39 Å. Waters were added in shells only to positive $F_o - F_c$ peaks greater than 3σ and that form at least one potential hydrogen bond with the protein or with other waters already hydrogen-bonded to the protein. Occupancies of the waters were refined during the last stages of refinement, and alternate conformations were included for residues Glu^{27}, Ile^{36}, Leu^{47}, Ser^{112}, and Leu^{151} of monomer A and Ile^{36} and Leu^{47} of monomer B. All waters in the refined model have B factors of less than 50 $Å^2$.
31. J. G. Navaza, *Acta Crystallogr.* **A50**, 157 (1994).
32. A. T. Brünger, personal communication.
33. L. M. Rice and A. T. Brünger, *Proteins* **19**, 277 (1994).
34. S. V. Evans, *J. Mol. Graph.* **11**, 134 (1993).
35. The electron density for the NH_2-terminal arm of AraC is better defined in monomer B; therefore, that monomer was used for generation of all sugar-binding figures.
36. K. E. van Holde and W. O. Weischet, *Biopolymers* **17**, 1387 (1978).

37. We thank A. Batchelor, E. Reisinger, J. Aishima, and M. Greisman for help with data collection; C. Ogata and R. Abramowitz of beamline X4A at the National Synchrotron Light Source for advice and technical support; and J. Berg, M. Amzel, and E. Lattman for comments on the manuscript. C. Becker, M. Nagypal, S. Jenkins, A. Favreau, M. Williams, and J. Withey helped with purification and crystallization efforts. We thank C. Turgeon and J. Hansen of the University of Texas Health Sciences Center at San Antonio for analyzing samples by analytical ultracentrifugation and A. Brünger and L. Rice for a prerelease version of X-PLOR for torsion angle dynamics refinement. Supported by the Howard Hughes Medical Institute (C.W. and beamline X4A), the David and Lucile Packard Foundation (C.W.), and grant GM18277 from the National Institutes of Health (R.S.). Atomic coordinates have been deposited at the Brookhaven Protein Data Bank (accession numbers 2ARC and 2ARA).

16 October 1996; accepted 18 February 1997

Quantitative Trait Loci for Refractoriness of *Anopheles gambiae* to *Plasmodium cynomolgi* B

Liangbiao Zheng, Anton J. Cornel, Rui Wang, Holger Erfle, Hartmut Voss, Wilhelm Ansorge, Fotis C. Kafatos, Frank H. Collins*

The severity of the malaria pandemic in the tropics is aggravated by the ongoing spread of parasite resistance to antimalarial drugs and mosquito resistance to insecticides. A strain of *Anopheles gambiae*, normally a major vector for human malaria in Africa, can encapsulate and kill the malaria parasites within a melanin-rich capsule in the mosquito midgut. Genetic mapping revealed one major and two minor quantitative trait loci (QTLs) for this encapsulation reaction. Understanding such antiparasite mechanisms in mosquitoes may lead to new strategies for malaria control.

Melanotic encapsulation, an immune reaction in which invading parasites are enclosed and destroyed within a melanin-rich capsule, is widespread among insects. Malaria parasites, which must develop into oocysts in the mosquito midgut, can also be encapsulated in some refractory vector strains, resulting in a block to disease transmission (*1*). The mechanism of parasite rejection is a key to the biology of interaction between *Plasmodium* and its vector, and an understanding of this mechanism may ultimately be useful in malaria control strategies such as mosquito population replacement using robust refractory strains.

Fully refractory and susceptible strains of *A. gambiae* have been selected for the ability to encapsulate or tolerate, respectively, oocysts of *Plasmodium cynomolgi*, a simian parasite. These strains respond similarly to most *Plasmodium* species, including the human pathogen *P. falciparum* (*1*). Many dif-

L. Zheng, R. Wang, H. Erfle, H. Voss, W. Ansorge, F. C. Kafatos, European Molecular Biology Laboratory, Meyerhofstrasse 1, 69117 Heidelberg, Germany.
A. J. Cornel and F. H. Collins, Centers for Disease Control and Prevention, 4770 Buford Highway, Mail Stop F22, Chamblee, GA 30341, USA.

*To whom correspondence should be addressed. E-mail: fhc1@cdc.gov

ferent paracentric chromosomal inversions are present in *A. gambiae* from both natural and laboratory-adapted strains (*2*). The previously described strains differ by a large paracentric inversion (*2La*) covering polytene divisions 23 through 26 of the left arm of chromosome 2. Refractoriness and susceptibility to *P. cynomolgi* B have been associated with the $2L+^a/+^a$ and *2La/a* karyotypes, respectively (*3*). To avoid the expected suppression of recombination by inversion polymorphism and to facilitate genetic analysis, we selected new refractory and susceptible strains bearing the same $2L+^a/+^a$ arrangement (*4*). Their reciprocal crosses yielded generally refractory F_1 female progeny; backcrosses (BCs) of reciprocal F_1 progeny revealed no sex-linked genetic component to parasite encapsulation (*5*). The BC of F_1 to the refractory strain produced progeny that were all highly refractory (Fig. 1A), indicating a dominant effect of the refractory allele (or alleles) of the loci involved (*6*).

BCs to the susceptible strain generated seven families (E1 through E7), with 19, 34, 36, 36, 25, 29, and 31 BC female progeny, that were blood-fed with infected *P. cynomolgi* B and then scored individually for intensity of infection and for encapsulation phenotype. Most of the BC progeny were either refractory or susceptible, which suggested that a single genetic locus is the major determinant of the encapsulation response (Fig. 1B). By contrast, the intensity of infection (normal plus encapsulated parasites) in the BC progeny varied broadly, which suggested that there is no simple genetic component of inheritance (Fig. 1C).

The microsatellite markers shown in Fig. 2 were heterozygous in the F_1 female parent and thus genetically informative. The marker genotypes in families E1 to E5 were correlated with the encapsulation phenotypes (*7*, *8*) by means of Mapmaker/QTL (*9*, *10*). When these five families were analyzed together, two QTLs were identified (Fig. 2). The major one (*Pen1*, for *Plasmodium* encapsulation 1) was identified near marker *H175*, with a combined LOD score of 22.7 that explains ~54% of the trait. A minor QTL (*Pen2*) was also identified near marker *H758*, with a LOD score of 4.1 that explains ~13% of the trait. By correlation of the genetic and cytogenetic maps with a subset of markers mapped by in situ hybridization to the polytene chromosomes (*2*, *5*, *7*), *Pen1* is probably located in division 8 of the right arm of chromosome 2 (2R), whereas *Pen2* is in or near division 43 of the left arm of chromosome 3 (3L). Progressively decreasing LOD scores in regions of the same

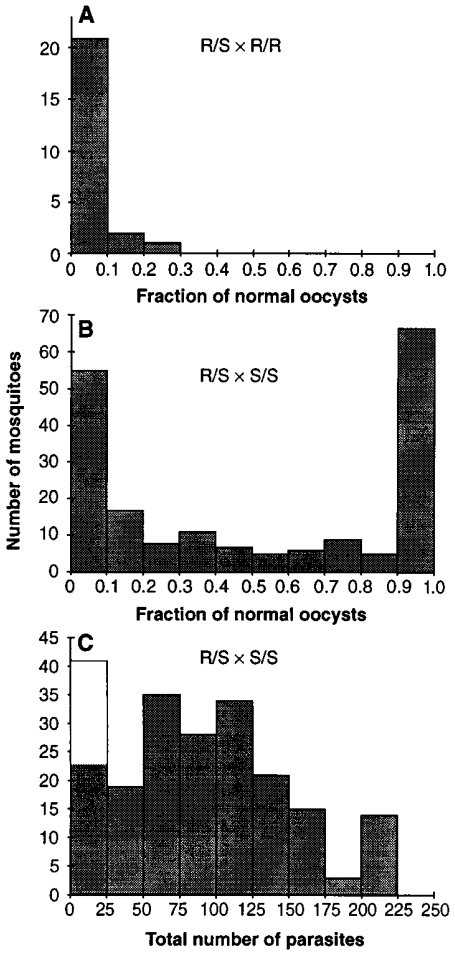

Fig. 1. Encapsulation of *P. cynomolgi* B is dominant and is controlled by a major locus. Distributions of traits are shown for BC female progeny from one family backcrossed to the refractory line (R/S × R/R) (**A**) and from the seven families backcrossed to the susceptible line (R/S × S/S) (**B** and **C**). Mosquitoes showing no infection could not be represented in (A) and (B) (*7* and *18*, respectively); they are shown as a white bar in (C).

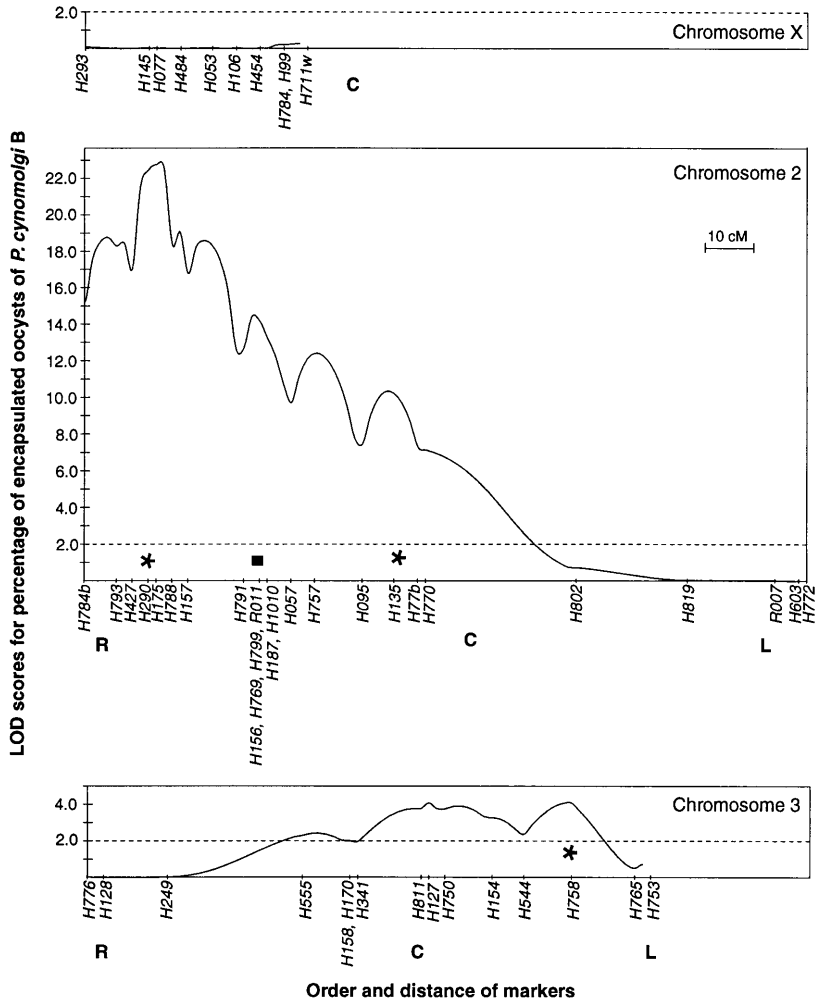

Fig. 2. QTLs controlling the encapsulation response to *P. cynomolgi* B. The genetic map was generated by genotyping 150 progeny from families E1 to E5. A few closely linked markers appeared in an order different from that in the standard map (*7*). Asterisks indicate locations of the encapsulation QTLs; ■ indicates a marginal peak in the infection LOD score (see Table 1). The approximate locations of the centromeres (C) and the arms of each chromosome (R, right; L, left) are labeled. Noninformative microsatellite markers are not shown.

chromosome away from each QTL are expected because of linkage. Secondary peaks were also observed, which, if significant, might indicate additional QTLs. Therefore, the whole genome was rescanned, with *Pen1* and *Pen2* both fixed (that is, assuming the presence of these two QTLs and mapping the residual variation). This revealed only one additional significant QTL, *Pen3*, which is near marker *H135* about 45 centimorgans (cM) from marker *H175* and probably near division 14 on 2R. The total contribution from these three QTLs amounted to 70% of the trait. By contrast, the X chromosome showed no influence on the refractoriness phenotype (Fig. 2).

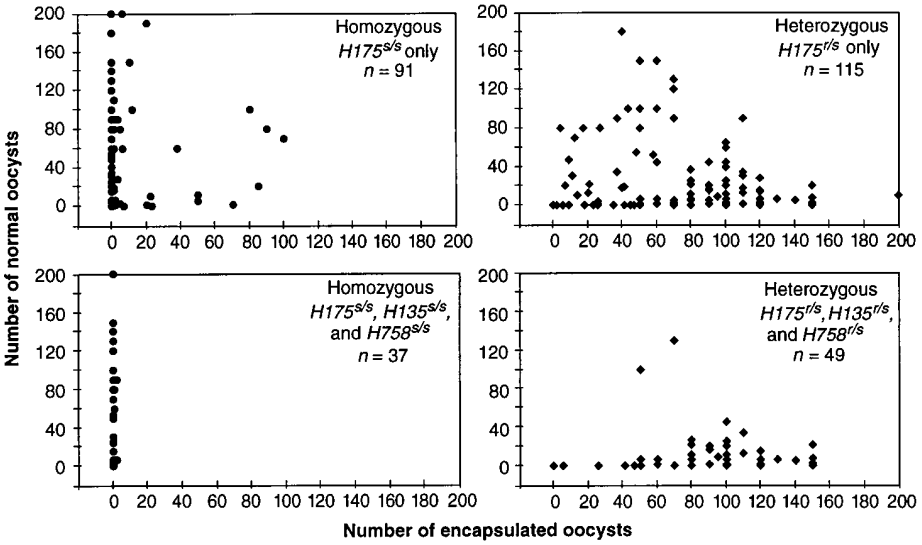

Fig. 3. In combination, the three QTLs control virtually completely the refractoriness to *P. cynomolgi* B. The numbers of normal and encapsulated oocysts in each mosquito are represented. Symbols ● and ◆ indicate homozygosity and heterozygosity, respectively, for the susceptible-derived allele only at marker *H175* (upper panels) or at markers *H175*, *H135*, and *H758* (lower panels). Note the substantial effect of the *H175* genotype alone (upper left versus upper right panel) and the additive effects of *H135* and *H758* (upper versus lower panels).

Table 1. *Pen1*, *Pen2*, and *Pen3* control the ability to encapsulate *P. cynomolgi* B oocysts. The underlined markers map closest to the three encapsulation QTLs; the boldface marker indicates a marginal peak in the infection LOD score (see Fig. 2). Numbers of progeny (out of 210 total from families E1 to E7) successfully genotyped for each marker and of progeny homozygous for the susceptible-derived alleles were subjected to a χ^2 test; significant deviations from the expected 1:1 ratio are indicated. Some genotypings failed for technical reasons; the E7 maternal parent was uninformative for marker *H788*.

Marker	Number of genotyped progeny	Number of homozygous progeny	χ^2 (df = 1)	LOD score (encapsulation)	LOD score (number of parasites)
		Chromosome 2			
H784b	208	102	0.08	21.56	0.38
H793	208	90	3.77	26.33	0.63
H427	210	91	3.73	24.30	0.40
H290	209	85	7.28†	30.99	1.32
H175	206	91	2.80	34.17	0.61
H788	177	73	5.43	28.51	1.34
H157	210	85	7.62†	26.49	1.17
H791	209	86	6.55*	20.61	2.12
H769	208	85	6.94†	24.41	2.38
R011	210	87	6.17*	24.90	2.02
H187	210	85	7.62†	21.32	2.23
H757	210	86	6.88†	22.06	1.92
H135	210	92	3.22	15.67	1.20
H770	209	97	1.08	12.38	1.43
H603	210	94	2.30	0.20	1.77
		Chromosome 3			
H758	204	107	0.49	5.91	0.00
H154	210	109	0.30	1.57	0.36
H127	210	106	0.02	4.19	0.62
H750	210	99	0.69	4.29	0.70
H158	209	104	0.00	2.61	0.70

*$0.025 > P > 0.010$. †$0.010 > P > 0.005$.

Both the refractory and susceptible strains are polymorphic for the *2Rbc* inversion, which encompasses polytene divisions 11B through 14A, and could affect the data for *Pen3*. We controlled for this variable by monitoring a nearby visible marker, *collarless* (*4*, *6*). All F_1 females were chosen to be *c*/*c*. Moreover, we reanalyzed data pooled from families derived from the same type of susceptible BC father, C/C (families E2, E3, and E6) or C/*c* (families E1, E4, and E5). In both cases, *Pen3* was identified, linked most closely with either *H135* or the next available marker, *H770*. Similarly, *Pen3* was identified near *H135* in family E7, which was derived from a *c*/*c* BC father and was analyzed using selected microsatellite markers. Thus, it is unlikely that the *2Rbc* inversion polymorphism explains any of the QTLs. Analysis of all seven families combined yielded similar results (Table 1). *Pen1* was located 1.5 cM from *H175* (LOD = 36.0) and contributed 60% of the trait; *Pen2* was mapped 8.0 cM from *H758* and contributed 19%. *Pen3* was identified 4.0 cM from *H135* when either *Pen1* alone or *Pen1* and *Pen2* were fixed. The combined actions of *Pen1*, *Pen2*, and *Pen3* appeared to control 76% of the trait.

These results were further validated by examining the distribution of infection and encapsulation phenotypes of genotypically sorted progeny (Fig. 3). Heterozygosity (the presence at marker *H175* of an allele derived from the refractory parent) conferred a certain degree of phenotypic refractoriness; the combined effect of refractory markers at all three loci was much stronger. Conversely, homozygosity (the absence of a refractory allele at these loci) resulted in mosquitoes that were completely, or in a few individuals almost completely, susceptible.

In contrast, no QTL was identified for the intensity of infection, except for a small peak (LOD = 2.38; 6% variance explained) near marker *H769* on chromosome 2 (Table 1). None of the refractoriness QTLs controlled the intensity of infection by *P. cynomolgi* B. Moreover, only a marginal deviation from the expected 1:1 ratio of homozygosity to heterozygosity in the BC progeny was observed, between but not at *Pen1* and *Pen3* (Table 1). This observation suggested that the QTLs were detrimental only to the parasites, not to the mosquito itself.

A genetic region that includes *Pen1* has been shown (*11*) to be involved in the

melanotic coating of abiotic Sephadex beads injected into the mosquito thorax (*12*). Interestingly, neither parasite nor bead encapsulation mapping experiments identified any locus within the *2La* region. The reported association of $2L+^a$ with refractoriness (*3*) may be an artifact of the previously available strains (for example, a result of suppression of recombination). It is also possible that a locus within the *2La* region is required for the expression of *Pen1*, *Pen2*, and *Pen3* but is not directly involved in encapsulation. The new strains are both $2L+^a/+^a$ and may already carry the same permissive allele at this locus.

Melanotic encapsulation is only one of several types of refractoriness of anopheline mosquitoes to *Plasmodium* parasites (*13*). Another common type is manifested earlier, before or during parasite invasion of the midgut epithelium (*14*). Two QTLs each have been identified for the susceptibility of *Aedes aegypti* mosquitoes to *P. gallinaceum* (*15*) and Brugian worms (*16*). However, these *Ae. aegypti* QTLs control the intensity of parasite infection and thus differ from the *Pen* loci of *A. gambiae*. Hence, our results establish that the development of malaria parasites can be blocked by two independent refractory mechanisms that are both temporally and functionally different.

The nature of *Pen1*, *Pen2*, and *Pen3* is not known, although *Pen3* maps in the general area where the prophenoloxidase gene is also located (*17*). In any case, the detailed localization of genes involved in the *A. gambiae* encapsulation response offers the opportunity to clone these genes positionally and to characterize the antiparasitic immune response of this vector at both the genetic and molecular levels.

REFERENCES AND NOTES

1. F. H. Collins *et al*., *Science* **234**, 607 (1986).
2. M. Coluzzi *et al*., *Trans. R. Soc. Trop. Med. Hyg.* **73**, 483 (1979).
3. K. D. Vernick and F. H. Collins, *Am. J. Trop. Med. Hyg.* **40**, 593 (1989); A. E. Crews-Oyen *et al*., *ibid.* **49**, 341 (1993).
4. The new refractory strain (L35) was derived from the previous one (*1*) and is homozygous for *collarless* (*7*). The new susceptible strain (4Ar/r) is homozygous for *pink-eye* and *red-eye* [C. B. Beard *et al*., *J. Hered.* **86**, 375 (1995)] and polymorphic for *collarless*. Both L35 and 4Ar/r are polymorphic for the *2Rbc* inversion but are fixed for $2L+^a$, *Xag* inversion of the X chromosome and the standard chromosome 3 karyotype.
5. F. H. Collins and A. J. Cornel, unpublished data.
6. Collarless (*c*/*c*) F_1 females were generated from a mass mating between L35 males and 4Ar/r females. Each was singly mated with one collared susceptible (either *C*/*c* or *C*/*C*), collarless susceptible (*c*/*c*), or collarless refractory male. These females were allowed to blood-feed on a *P. cynomolgi* B–infected rhesus monkey. After a single oviposition, the normal and encapsulated oocysts in the midgut of each female were counted 5 to 6 days later. The heterozygosity of some microsatellite markers in the susceptible strain allowed mapping of *collarless* in families E4 and E5 (*7*). Each BC family was individually reared, and the emerging females were allowed to blood-feed on another infected rhesus monkey. Infection and encapsulation phenotypes of the midgut were determined as above. The remaining carcasses were frozen for genomic DNA preparation and microsatellite genotyping.
7. L. Zheng, F. H. Collins, V. Kumar, F. C. Kafatos, *Science* **261**, 605 (1993); G. Dimopoulos *et al*., *Genetics* **143**, 953 (1996); L. Zheng, M. Q. Benedict, A. Cornel, F. H. Collins, F. C. Kafatos, *ibid.*, p. 941.
8. Fluorescent microsatellite genotyping was carried out as described [D. C. Mansfield *et al*., *Genomics* **24**, 225 (1994)] with an ALF DNA sequencer (Pharmacia). The data were analyzed with Fragment Manager (Pharmacia). Genotyping of randomly selected mosquitoes was repeated to verify the quality of the data.
9. E. Lander *et al*., *Genomics* **1**, 174 (1987); A. Paterson *et al*., *Nature* **335**, 721 (1988).
10. A genetic map was generated from the combined genotype data from families E1 to E5. QTL mapping was performed on individual and combined families E1 to E5 with the markers shown in Fig. 2 and for selected markers on E6 and E7. A LOD score of 3.0 was used as the minimum for declaring the existence of a QTL. After the highest value QTLs in chromosomes 2 and 3 (*Pen1* and *Pen2*) were fixed, the residual variations were mapped, revealing only one additional significant QTL, *Pen3*. Maximum likelihood estimates were also calculated in families E1 to E7 for markers listed in Table 1 (*9*). A similar genetic map order was also obtained with the program Joinmap [P. Stam, *Plant J.* **5**, 739 (1993)].
11. M. J. Gorman *et al*., *Genetics*, in press.
12. M. J. Gorman *et al*., *Exp. Parasitol*. **84**, 380 (1996).
13. A. Warburg and L. H. Miller, *Parasitol. Today* **7**, 179 (1991).
14. H. M. Al-Mashhadani, G. Davidson, C. F. Curtis, *Trans. R. Soc. Trop. Med. Hyg.* **74**, 585 (1980); P. M. Graves and C. F. Curtis, *Ann. Trop. Med. Parasitol.* **76**, 633 (1982); M. Shahabuddin *et al*., *Exp. Parasitol.* **81**, 386 (1995); K. D. Vernick *et al*., *ibid.* **80**, 583 (1995).
15. W. L. Kilama and G. B. Craig Jr., *Ann. Trop. Med. Parasitol.* **63**, 419 (1969); D. W. Severson *et al*., *Genetics* **139**, 1711 (1995).
16. W. W. MacDonald and C. P. Ramachandran, *Ann. Trop. Med. Parasitol.* **59**, 64 (1965); D. W. Severson *et al*., *Insect Mol. Biol.* **3**, 67 (1994).
17. W.-J. Lee *et al*., unpublished data.

18. We thank S. Winkler, C. Schwager, R. Saffrich, U. Nentwich, and J. Stegemann for help in genotyping, and W. Collins, J. Sullivan, and C. Morris for help with rhesus monkeys. Supported by the John D. and Catherine T. MacArthur Foundation and the UNDP/World Bank/WHO Special Programme for Research and Training in Tropical Diseases (TDR). Experiments with rhesus monkeys were performed under the guidelines of CDC animal use protocol 676-COL-MON-CH.

26 December 1996; accepted 26 February 1997

Prevention of Lysosomal Storage in Tay-Sachs Mice Treated with *N*-Butyldeoxynojirimycin

Frances M. Platt,* Gabrielle R. Neises, Gabriele Reinkensmeier, Mandy J. Townsend, V. Hugh Perry, Richard L. Proia, Bryan Winchester, Raymond A. Dwek, Terry D. Butters

The glycosphingolipid (GSL) lysosomal storage diseases result from the inheritance of defects in the genes encoding the enzymes required for catabolism of GSLs within lysosomes. A strategy for the treatment of these diseases, based on an inhibitor of GSL biosynthesis *N*-butyldeoxynojirimycin, was evaluated in a mouse model of Tay-Sachs disease. When Tay-Sachs mice were treated with *N*-butyldeoxynojirimycin, the accumulation of G_{M2} in the brain was prevented, with the number of storage neurons and the quantity of ganglioside stored per cell markedly reduced. Thus, limiting the biosynthesis of the substrate (G_{M2}) for the defective enzyme (β-hexosaminidase A) prevents GSL accumulation and the neuropathology associated with its lysosomal storage.

The GSL storage diseases (*1*) result from the inheritance of defects in the genes encoding the catabolic enzymes required for the complete breakdown of GSLs within lysosomes. Possible strategies for the treatment of these debilitating and often fatal diseases include enzyme replacement therapy, gene therapy, substrate deprivation, allogeneic bone marrow transplantation, and palliative measures (*2*). Of these, symptomatic management is the only approach for treating most of these disorders, although transplantation techniques have been applied to some of these diseases. Currently, only the type 1 form of Gaucher disease, which is characterized by glucocerebrosidase deficiency in the absence of neuropathology, has been successfully treated by enzyme replacement therapy (*3*, *4*). However, skeletal abnormalities associated with the disease respond slowly to this treatment (*4*), and the neuropathologic forms of the

F. M. Platt, G. Reinkensmeier, R. A. Dwek, T. D. Butters, Glycobiology Institute, Department of Biochemistry, University of Oxford, South Parks Road, Oxford 0X1 3QU, UK.
G. R. Neises, Monsanto Company, 700 Chesterfield Village Parkway, St. Louis, MO 63198, USA.
M. J. Townsend and V. H. Perry, Department of Pharmacology, University of Oxford, Mansfield Road, Oxford OX1 3QT, UK.
R. L. Proia, National Institute of Diabetes and Digestive and Kidney Diseases, National Institutes of Health, Bethesda, MD 20892, USA.
B. Winchester, Institute of Child Health, 30 Guilford Street, London WC1N 1EH, UK.

*To whom correspondence should be addressed. E-mail: fran@oxglua.glycob.ox.ac.uk